*ADVANCES IN CHEMICAL PHYSICS, 2025, Vol. 44, No. 1, pp. 54–66*

## COMBUSTION, EXPLOSION AND SHOCK WAVES

# EFFECT OF ADDITIVE MODIFIERS ON THE COMBUSTION CHARACTERISTICS OF COMPOSITE ALUMINIZED PROPELLANTS

**© 2025 O. G. Glotov[a, b, *], N. S. Belousova[a, b]**

[a] *Voevodsky Institute of Chemical Kinetics and Combustion Siberian Branch of the Russian Academy of Sciences, Novosibirsk, Russia*

[b] *Novosibirsk State Technical University, Novosibirsk, Russia*

**e-mail: glotov@kinetics.nsc.ru*

Received February 07, 2024

Revised March 24, 2024

Accepted April 22, 2024

**Abstract.** The effect of $TiB_2$, $AlMgB_{14}$, $(NH_4)_2TiF_6$, $NH_4BF_4$ and $Ca_3(PO_4)_2$ additives-modifiers on the combustion parameters of composite propellants based on ammonium perchlorate (about 60%), powdered aluminum (about 20%), and a binder of the methylpolyvinyl tetrazole type (about 20%) was studied. The additives were introduced in an amount of about 2%. The burning rates of the propellants were measured and the condensed combustion products were studied at a pressure of 0.35 MPa. The effect of additives was assessed in terms of their influence on the burning rate, as well as on the mass, size and incompleteness of combustion of agglomerates. The most effective additives were $TiB_2$ and $AlMgB_{14}$. Conclusions were made on the possibility of regulating the specified combustion parameters by introducing small additives into the propellant and on the need for further research in this direction.

**Keywords:** *model composite propellant, aluminum, additives, combustion modifiers, titanium diboride, aluminum-magnesium boride, ammonium tetrafluoroborate, ammonium-titanium fluoride, calcium phosphate 3-substituted, burning rate, agglomeration, condensed combustion products, sampling method, agglomerates, oxide particles, granulometric composition, combustion completeness*

**DOI:** 10.31857/S0207401X250107e1

## 1. INTRODUCTION

The development of rocket technology is partly ensured by the improvement of fuel formulations. The purpose of rocket propellant is to release the required amount of energy and working fluid at a given rete during combustion under certain conditions. To date, many effective combustibles, oxidizers and binders are known [1–4], with a special place occupied by composite propellants containing metal particles as a fuel [5–7]. Aluminum has become the most widely used due to the successful combination of such qualities as high heat of combustion and density, safety of handling powder, harmlessness of combustion products, and commercial availability. However, aluminum is characterized by the phenomenon of agglomeration [8], which consists in the unification and merging of the original particles into agglomerates in the combustion wave. Agglomeration usually leads to undesirable consequences – a decrease in the completeness of metal combustion, accumulation of slag in the engine chamber, etc. Therefore, the search for ways to reduce agglomeration is the subject of many experimental studies. The main factors that affect the agglomeration and combustion of aluminum in the composition of propellants are listed below.

The formulation factors are the aluminum content [9–11], the granulometric composition of the components [9, 12], the nature of the binder [13–16], the presence of nitramines [17–19], ammonium nitrate [20–23] or other alternative oxidizers [24–29]. The physical factors are the pressure [30] and the burning rate [31]. The burning rate depends on the pressure and dispersion of ammonium perchlorate (AP) [11, 31], therefore, in order to reduce agglomeration while simultaneously meeting other propellant requirements, it is necessary to optimize a complex system with numerous direct and reverse dependesies. The following are promising

ways of influencing the behavior of the metal in the combustion wave, including agglomeration: modification of the properties of the metal in the volume, for example, by introducing a second metal [32–34]; preparetion of composite particles [35, 36]; modification of the particle surface or the oxide layer covering it [35, 37–44]; introduction of additives into the propellant composition [24, 45–47]. In this case, the introduction of nanosized aluminum [48, 49] can be considered both as an additive to the propellant and as a modification of the properties of aluminum. General ideas about the mechanism of action of additives introduced into the propellant or directly into the metal particles are presented in [50].

This work is aimed at experimentally assessing the effect of five additives on aluminum agglomeration in a typical propellant formulation with AP and an active binder. The essence of the work is to test the possibility of achieving beneficial effects by introducing additives. With regard to agglomeration, these include a decrease in the size and mass of large agglomerate particles, an increase in the completeness of metal combustion, and a decrease in the size of small oxide particles. The work is exploratory in nature and was performed using a simplified method for sampling combustion products. More detailed studies, in particular, of the mechanisms of action of additives, make sense only if the desired effects are detected.

## 2. PROPELLANTS AND ADDITIVES UNDER STUDY

The experiments were carried out with uncured model mixtures that had a paste-like consistency and contained the following components: Ammonium perchlorate of one of two fractions – coarse with particle sizes of 500–630 μm (APc), or medium with particle sizes of 180–250 μm (AP); active fuel-binder – methylpolyvinyltetrazole (MPVT) type [20]; micron-sized aluminum powder of the ASD-4 brand (Al). The mass ratio of the components AP/binder/Al = 60/20/20 or 62/20/18. The procedure for preparing the propellant mass samples included weighing the components on an MV 210-A analytical balance with an accuracy of 0.0001 g and mixing them manually in a bronze cup with a fluoroplastic spatula. When working with the spatula, they acted very carefully so as not to crumble of the large AP particles. The typical mass of the prepared portion of propellant is approximately 5 g, and in such a portion it is easy to visually control the homogeneity of mixing.

The granulometric characteristics of the powder components are presented in Table 1 and Fig. 1 in the form of normalized functions of the density distribution of the relative mass of particles by size. The normalization was carried out in such a way that the area under the curve (mass) was equal to 1.

The mean particle sizes of the powders $D_{mn}$ were calculated using the formula

$$D_{mn} = {}_{m-n}\sqrt{\left(\sum_{i=1}^{k} D_i^m \cdot N_i\right) \Big/ \left(\sum_{i=1}^{k} D_i^n \cdot N_i\right)}, \quad (1)$$

where $m$, $n$ are integers specifying the order of the mean size, $k$ is the number of size intervals in the histogram, $N_i$ is the number of particles in the $i$-th interval, $D_i$ is the middle of the $i$-th interval. From here on, the calculated values of the mean diameters are given without rounding.

The scheme of variation of propellant compositions is presented in Fig. 2. There are base propellants P1, P2 and P3. Propellant P1 contains 20% of binder, 20% of Al and 60% of APc. Propellant P2 differs in the size of oxidizer particles and contains 20% of binder, 20% of Al and 60% of AP. Propellant P3 has a reduced Al content (18%), an increased AP content (62%) and the same amount of binder (20%). Following [51], additives-modifiers were introduced into each base propellant in an amount of about 2% (over 100%). Additives: titanium diboride $TiB_2$, aluminum and magnesium boride $AlMgB_{14}$, ammonium titanium(IV) fluoride $(NH_4)_2TiF_6$, ammonium tetrafluoroborate $NH_4BF_4$, calcium phosphate 3-substituted $Ca_3(PO_4)_2$. The choice of additives is due to the presence of "combustible" atoms of Al, Mg, B, Ti or an F atom as an oxidizer and at the same time an element capable of interacting with the oxide film covering aluminum particles. The compound $Ca_3(PO_4)_2$ is conditionally inert and is used for comparison. Below we will discuss three "lines" of formulation obtained from base propellants P1, P2 and P3 by introducing the listed

**Table 1.** Mean particle sizes of powdered propellant components (in μm)

| Propellant | $D_{10}$ | $D_{30}$ | $D_{32}$ | $D_{43}$ |
|---|---|---|---|---|
| APc | 712 | 723 | 734 | 746 |
| AP | 221 | 232 | 242 | 249 |
| Al | 4.2 | 5.8 | 8.7 | 15 |

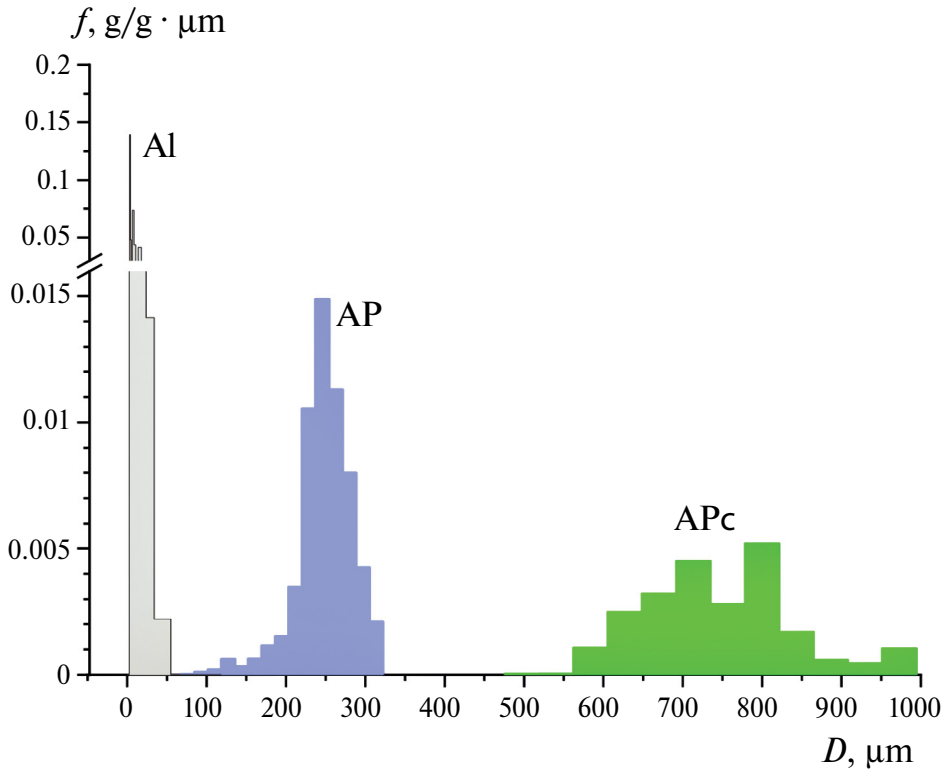


**Fig. 1.** Mass distribution functions of aluminum, coarse (APc) and medium (AP) ammonium perchlorate particles by size.

**Table 2. Component composition (%.wt) of the studied propellants**

| Fuel | Binder | Al | APc | AP | $AlMgB1_4$ | $TiB_2$ | $NH_4BF_4$ | $(NH4)_2TiF_6$ | $Ca_3(PO_4)_2$ |
|---|---|---|---|---|---|---|---|---|---|
| P1 | 20 | 20 | 60 | – | – | – | – | – | – |
| P11 | 20 | 20 | 60 | – | 2 | – | – | – | – |
| P12 | 20 | 20 | 60 | – | – | 2 | – | – | – |
| P13 | 20 | 20 | 60 | – | – | – | 2 | – | – |
| P14 | 20 | 20 | 60 | – | – | – | – | 2 | – |
| P15 | 20 | 20 | 60 | – | – | – | – | – | 2 |
| P2 | 20 | 20 | – | 60 | – | – | – | – | – |
| P21 | 20 | 20 | – | 60 | 1.6 | | | | |
| P22 | 20 | 20 | – | 60 | | 1.8 | – | – | – |
| P23 | 20 | 20 | – | 60 | – | – | 2 | – | – |
| P24 | 20 | 20 | – | 60 | – | – | – | 2.1 | – |
| P25 | 20 | 20 | – | 60 | – | – | – | – | 2.5 |
| P3 | 20 | 18 | – | 62 | – | – | – | – | – |
| P31 | 20 | 18 | – | 62 | 2 | – | – | – | – |
| P32 | 20 | 18 | – | 62 | | 1.5 | | | |
| P33 | 20 | 18 | – | 62 | – | – | 2.4 | – | – |
| P34 | 20 | 18 | – | 62 | – | – | – | 1.5 | – |
| P35 | 20 | 18 | – | 62 | – | – | – | – | 2.2 |

*Note:* Additives were introduced in excess of 100%

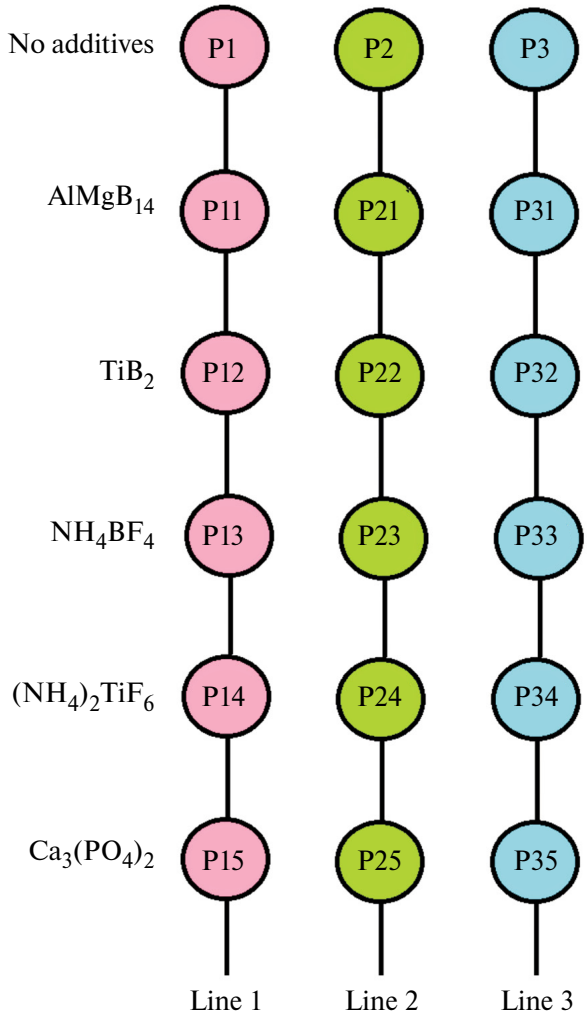


**Fig. 2.** Scheme of variation of propellant composition.

additives (Fig. 2). The compositions of the model propellants are presented in Table 2.

## 3. CONDUCTING AND PROCESSING THE RESULTS OF EXPERIMENTS

The experimental method is based on burning the test propellant sample in a small high-pressure vessel (mini-bomb) at a pressure of 0.35 MPa in nitrogen. At the same time, the combustion process is video-recorded through windows and condensed combustion products (CCP) are collected into the liquid.

The appearance of the high-pressure vessel (mini-bomb) is shown in Fig. 3. The outer diameter of the body is 90 mm, the effective diameter of the windows is 30 mm, the working pressure is up to 3 MPa, the volume is 0.33 L.

The sample is ignited using a nichrome wire heated by an electric current. A glass with a "freezing" liquid, distilled water, is placed under the sample. The glass diameter is 0.5 mm smaller than the inner diameter of the vessel. The sample in the form of a paste-like mixture is placed in a plexiglass cup with an inner diameter of 5 mm and a depth of 5 mm and fixed in the vessel so that the combustion torch is directed downwards. The distance from the surface of the sample to the surface of the liquid before the experiment was 1.5 cm. The pressure is created by gas from a cylinder and controlled by a manometer. The combustion process of the sample is recorded using a video camera. Burning metal particles-agglomerates flying out of the surface of the sample go out upon entering the liquid. Oxide particles in the free volume of the high-pressure vessel after combustion of the sample, upon sufficiently long exposure, settle on the surface of the liquid. The table 3 presents the results of the assessment of the velocity and time of settling of particles with a density of 3.7 g/cm$^3$ (aluminum oxide) in gas at a pressure of 0.35 MPa. The calculations were carried out using the AeroCalc aerosol calculator [52] to determine the holding time. The settling distance is 65 mm, which corresponds to the height of the free volume of the vessel, equal to the distance from the liquid surface to the top lid. The settling time was determined as the quotient of division the distance and the settling velocity. The settling velocity of spherical particles with a diameter of 2.2 μm and a density of 3.7 g/cm$^3$ is 0.54 mm/s. They will cover a distance of 65 mm in 120 s. The gas suspension was held in the vessel for 5 min so that particles larger than 2 μm guaranteed to have settled into the liquid.

Thus, in the conducted experiments, the agglomerates leaving the burning surface of the sample

**Table 3.** Estimation of the velocity and time of settling of particles in gas

| Particle diameter, μm | Sedimentation velocity, mm/s | Re number | Sedimentation time, s |
|---|---|---|---|
| 10 | 11.2 | 0.026 | 5.8 |
| 5 | 2.8 | 0.0032 | 23 |
| 3 | 1 | 0.0007 | 65 |
| 2.5 | 0.7 | 0.004 | 92 |
| 2.2 | 0.54 | 0.0027 | 120 |
| 2 | 0.4 | 0.0026 | 163 |

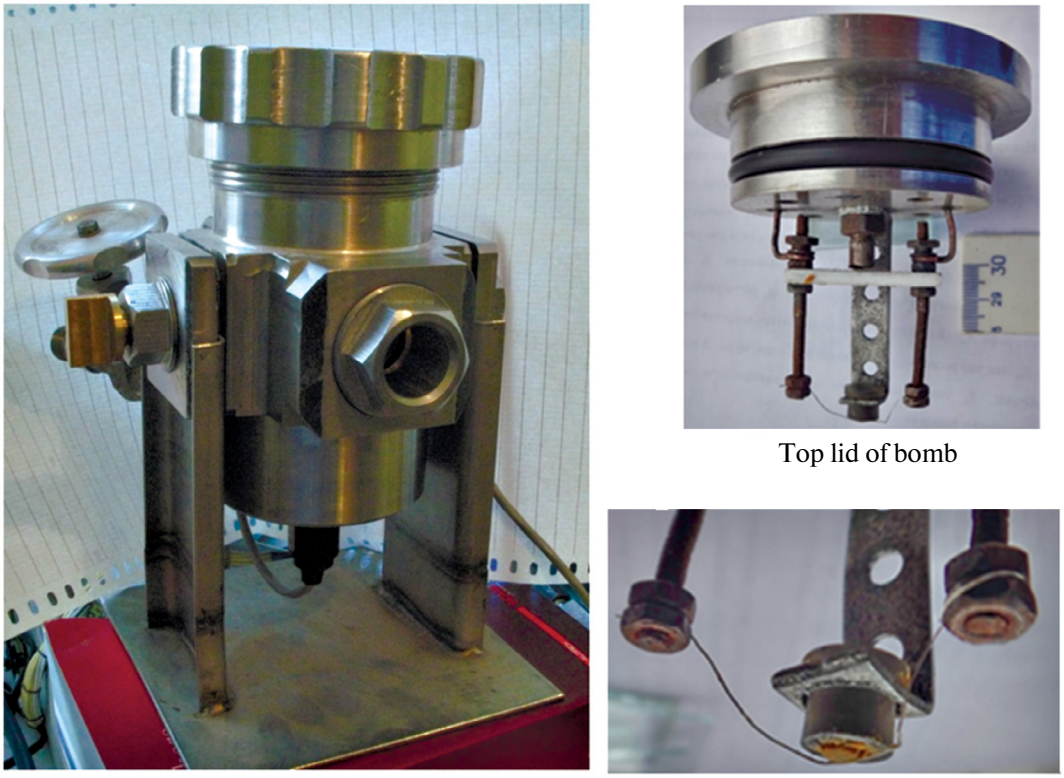

General external appearance

Top lid of bomb

Sample with igniting wire

**Fig. 3.** Photographs of a high-pressure vessel (mini-bomb) and its equipment.

are quenched and completely sampled. Oxide particles are not completely trapped. Some amount of oxide particles smaller than 2 μm exit with the gas when the pressure is released after the experiment. The "mass average" $D_{43}$ was used as a characteristic size of the agglomerates, and the "surface average" $d_{32}$ was used for the oxide particles. The specified sizes were calculated using formula (1).

## 4. PREPARATION AND ANALYSIS OF SAMPLED CCP PARTICLES

After removing the sampling glass, the suspension in it was filtered through a wire sieve with a mesh size of 80 μm. Particles larger than 80 μm were considered agglomerates. It is assumed that the boundary size $D_L$ separating agglomerates and oxide particles depends on the propellant formulation and combustion conditions [53]. There are various values of $D_L$ in the literature. For example, in [54, 55] agglomerates were considered to be particles larger than 30 μm, in [56] $D_L$ = 49 μm was taken, in [17] the size of $D_L$ was 119 μm. In this work, $D_L$ = 80 μm is accepted as a certain "universal" value, justified also by considerations of practical convenience – "wet" sifting of an aqueous suspension of particles through an 80 μm sieve is carried out quite easily. The residue on the sieve was dried at room temperature, weighed and the dimensionless mass of the agglomerates $m_{80}$ was determined as a relation the mass of particles larger than 80 μm to the mass of the propellant sample before the experiment.The absolute error in determining the value of $m_{80}$ usually does not exceed 0.02.

The dried agglomerate particles were subjected to morphological, granulometric and chemical analyses. The morphology of the particles was studied under an MBS-10 optical microscope with a DCM-300 ocular camera. Particle size analysis was carried out using an Pictoval optical projection microscope (Carl Zeiss Jena, Germany) and a semi-automatic 23-channel counting device with measuring circles on a transparent template ruler [57, 58]. The absolute error in measuring the particle diameters is ±22 μm. The incompleteness of agglomerates combustion was determined by the cerimetric method of analytical chemistry [59, 60] using reducing number *RN*, which characterizes the ability of a material

to attach oxygen, that is, to oxidize. The measure of incompleteness of combustion $\eta$ is the ratio of the $RN$ numbers after combustion, that is, $RN_{ccp}$ for combustion products, and $RN_{prop}$ for propellant. The reducing number for CCP $RN_{ccp}$ is calculated taking into account the mass of agglomerates:

$$RN_{ccp} = (RN \text{ for agglomerates}) \cdot m_{80}. \quad (2)$$

The reducing number for propellant $RN_{prop}$ is calculated as the product of the reducing number for metallic fuel $RN_{mf}$ determined as a result of chemical analysis and the mass fraction of metallic fuel $m_{mf}$ in the propellant:

$$RN_{prop} = RN_{mf} \cdot m_{mf}. \quad (3)$$

As a result, the incompleteness of agglomerate combustion:

$$\eta = RN_{ccp}/RN_{prop}. \quad (4)$$

In this definition, incompleteness of combustion can vary from 1 (nothing burned) to 0 (everything burned). The ratio of the measured $RN_{mf}$ and its theoretical value gives an idea of the "degradation" of the metallic fuel. For the used ASD-4 $RN = 10.14 \pm 0.28$ (averaged over 6 samples), while the theoretical value for aluminum is 11.12 [60]. The value 10.14/11.12 = 0.912, or 91.2%, can be interpreted as the content of active (unoxidized) metal in the original aluminum. The value $m_{mf} = 0.2$ for propellants of lines 1 and 2 and $m_{mf} = 0.18$ for propellants of line 3. Relative error of determination $\eta$ typically 5%-7%.

The "pass" through the 80 μm sieve – a suspension of fine oxide particles in water – was analyzed on an automatic granulometer "Malvern-3600E" (Great Britain). Mode: size range 0.5–118 μm, ultrasonic treatment of suspension within 30 s before measurement, mechanical stirrer is on during measurement. Each sample was analyzed twice. The measurement was repeated after 3 minutes, the results were averaged. Relative measurement error of the sizes – 10%.

Based on the obtained empirical size distribution functions, we calculated mean diameters of fine oxide particles $d_{mn}$ and agglomerate particles $D_{mn}$ according to formula (1) in the ranges of 0.5–80 μm and 80–$D_{max}$, respectively. Here $D_{max}$ is the right boundary of the last histogram interval in the distribution function of agglomerates.

Sample burning rate ($r$, mm/s) determined by dividing the length of the sample by its burning time. The length of the sample is the depth of the cup 5 mm; the burning time was determined by processing video recordings of the combustion process. The absolute error in determining the burning rate is 0.1 mm/s. Fig. 4 shows frames from a video recording of the sample combustion process.

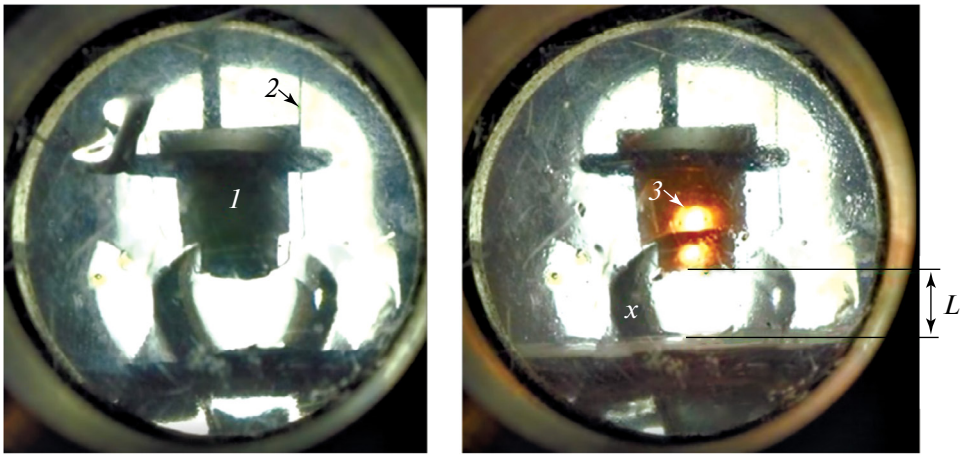


**Fig. 4.** Video footage of the combustion process of a miniature sample in a mini-bomb for the collection of combustion product particles. Shooting in the passing background light with illumination through the rear window of bomb: Left frame – view before combustion, right frame – during combustion: 1 – sample in a plexiglass cup, fixed to a bracket; 2 – ignition wire; 3 – burning surface. It is visible that it has shifted from the cut of the cup inward (upward); $x$ – one of the parasitic reflections that form on the edges of the glass with freezing liquid; $L$ – distance from the sample to the surface of the liquid before ignition of the sample.

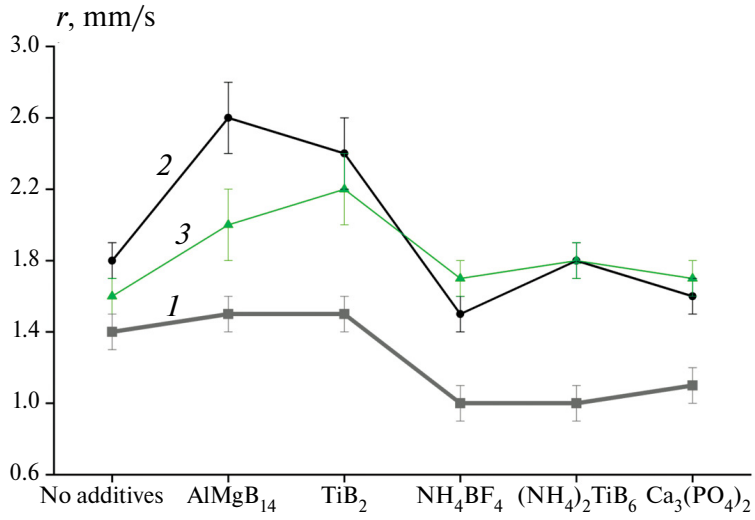


**Fig. 5.** Burning rates of the studied propellants at a pressure of 0.35 MPa: numbers 1, 2, 3 – correspond to propellants of lines 1, 2, 3.

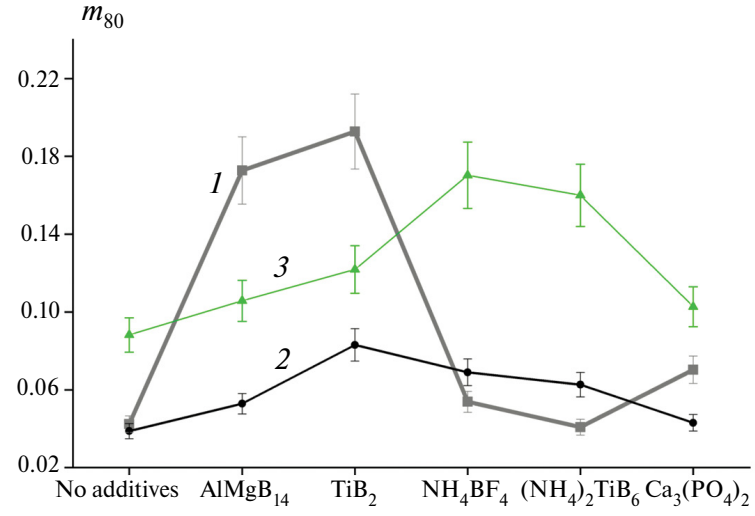


**Fig. 6.** Dimensionless mass $m_{80}$ of agglomerate particles: numbers 1, 2, 3 – correspond to propellants of lines 1, 2, 3.

## 5. RESULTS AND DISCUSSION

### *5.1. Burning rate*

Fig. 5 shows the burning rate levels of propellants with additives – modifiers. The additive formulas are signed under the abscissa axis, the burning rate is plotted along the ordinate axis. The points belonging to each of the three formula lines are connected.

As can be seen, the additives $AlMgB_{14}$ and $TiB_2$ increase the burning rate, while the additives $Ca_3(PO_4)_2$, $(NH_4)_2TiF_6$, $NH_4BF_4$ mainly decrease the burning rate compared to the corresponding base propellants. Here the words "mainly" are used due to the fact that the effect of the last three additives is ambiguous for different formulation lines. For propellants of line 3, the additives $Ca_3(PO_4)_2$, $(NH_4)_2TiF_6$, $NH_4BF_4$ have a weak effect on the burning rate, but still slightly (within the error) increase the rate.

### *5.2. Mass and size of agglomerates*

The mass of agglomerates is characterized by a dimensionless parameter $m_{80}$ (see Fig. 6). From this figure it can be seen that for propellants of lines 1, 2 and 3 all the studied additives lead to an increase in the mass of $m_{80}$ agglomerates, with the exception of the additive $(NH_4)_2TiF_6$ for propellant of line 1.

Table 4 shows the mean sizes of agglomerates $D_{mn}$. Fig. 7 shows the effect of additives on the agglomerate mean size $D_{43}$.

The effect of additives in different propellant lines is ambiguous. Let us note the cases of the desired effect – reduction of $D_{43}$. For propellants of line 1, additives

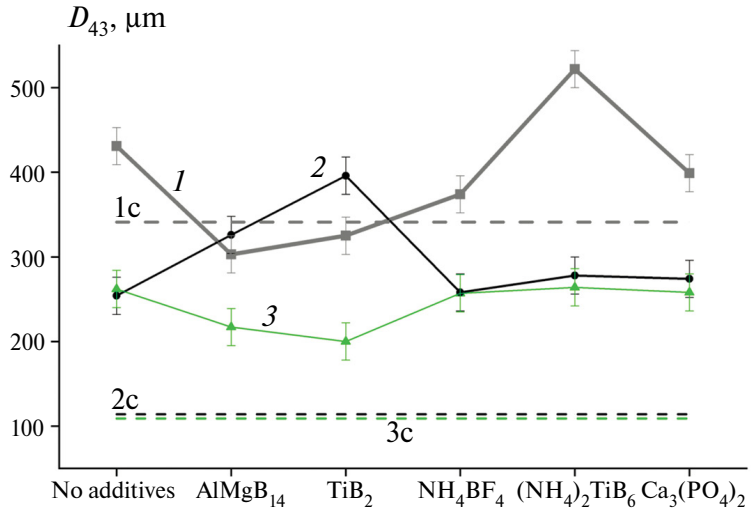


**Fig. 7.** Mean sizes of $D_{43}$ agglomerate particles: broken curves 1, 2, 3 correspond to propellants of lines 1, 2, 3; horizontal dotted lines 1c, 2c, 3c – calculation according to model [57] for propellants of lines 1, 2, 3.

**Table 4.** Mean sizes $D_{mn}$ of agglomerates (in μm)

| Propellant | $D_{10}$ | $D_{30}$ | $D_{32}$ | $D_{43}$ | $D_{53}$ |
|---|---|---|---|---|---|
| P1 | 246 | 306 | 373 | 431 | 457 |
| P11 | 225 | 252 | 279 | 303 | 214 |
| P12 | 245 | 272 | 301 | 325 | 336 |
| P13 | 268 | 304 | 341 | 374 | 390 |
| P14 | 310 | 376 | 453 | 522 | 551 |
| P15 | 281 | 316 | 355 | 399 | 422 |
| P2 | 186 | 210 | 235 | 254 | 263 |
| P21 | 234 | 267 | 300 | 326 | 338 |
| P22 | 267 | 307 | 350 | 396 | 420 |
| P23 | 197 | 219 | 240 | 258 | 265 |
| P24 | 212 | 235 | 258 | 278 | 287 |
| P25 | 214 | 235 | 257 | 274 | 282 |
| P3 | 157 | 194 | 234 | 262 | 274 |
| P31 | 135 | 160 | 188 | 217 | 232 |
| P32 | 138 | 161 | 184 | 200 | 206 |
| P33 | 183 | 209 | 236 | 257 | 267 |
| P34 | 191 | 214 | 237 | 258 | 267 |
| P35 | 171 | 193 | 216 | 232 | 239 |

of $AlMgB_{14}$ and $TiB_2$ lead to a noticeable reduction of $D_{43}$, additives $NH_4BF_4$ and $Ca_3(PO_4)_2$ – to a slight decrease. For propellants of line 2, no additive led to a decrease in $D_{43}$. For propellants of line 3, additives of $AlMgB_{14}$ and $TiB_2$ lead to a decrease in $D_{43}$.

For comparison, the maximum possible agglomerate size was calculated using the tetrahedral pocket model [61], in which the pocket parameters and agglomerate size are calculated assuming that large oxidizer particles are located at the vertices of a regular tetrahedron. The internal volume of the tetrahedron is filled with a mixture of binder and metal and forms a pocket that generates an agglomerate. The calculated agglomerate size for propellants of lines 1, 2, 3 is 341 μm, 114 μm and 109 μm, respectively. As can be seen from Fig. 7, the experimental values for propellants of lines 2 and 3 significantly exceed the calculated ones, which indicates an "interpocket" [11] agglomeration mechanism. The model works better for propellants of line 1 with coarse AP. In this case, for three of the additives under consideration, the relative difference between the calculated and experimental values of $D_{43}$ is 13%, 5% and 9% for propellants P11, P12 and P13, respectively. This indicates the suppression of "interpocket" agglomeration by the additives $AlMgB_{14}$, $TiB_2$, $(NH_4)_2TiF_6$.

### *5.3. The agglomerate combustion incompleteness of and sizes of oxide particles*

Values of agglomerate combustion incompleteness for the studied propellants, $\eta$, versus the type of additives are presented in Fig. 8. Analysis of the data in Fig. 8 shows the following. For propellants of lines 1 and 3 only additive $Ca_3(PO_4)_2$ somewhat reduces the incompleteness of combustion $\eta$. For propellants of line 2, the value of $\eta$ is reduced by additives $(NH_4)_2TiF_6$ and $Ca_3(PO_4)_2$.

Fig. 9 shows the results of the effect of additives on the $d_{32}$ sizes of fine particles. Chemical analysis

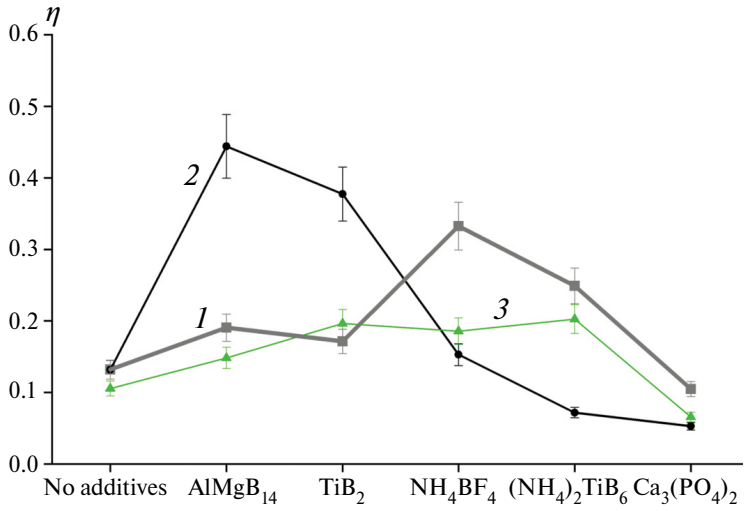


**Fig. 8.** Change in combustion incompleteness $\eta$: numbers 1, 2, 3 correspond to propellant lines 1, 2, 3.

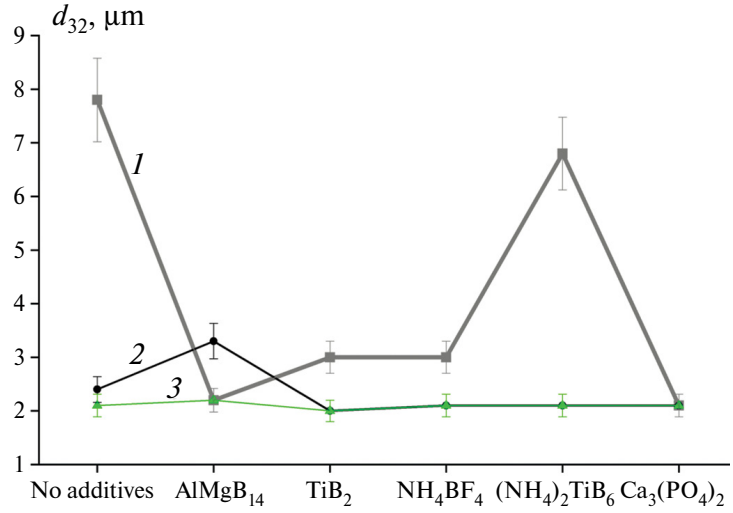


**Fig. 9.** Comparison of fine particle sizes $d_{32}$: curve numbers 1, 2, 3 correspond to the propellants of lines 1, 2, 3.

of these particles was not carried out, since it is expected that these particles are predominantly oxide [14].

The mean size $d_{32}$ of oxide particles in most cases is in the range of 2–3.5 μm and changes slightly with the introduction of additives. The "outliers" for line 1 propellants (base and propellant with the additive $(NH_4)_2TiF_6$ are probably due to the peculiarities of particle preparation. At the initial stage of the studies, we did not pay due attention to strict adherence to the holding time of the gas suspension in the bomb. Insufficient holding time could lead to incomplete sedimentation of relatively small particles in the liquid, their subsequent loss during the release of gas from the bomb, and, as a consequence, to an overestimated value of the mean particle size that had time to settle in the liquid. Without taking into account the "outliers", we note the multidirectional influence of the $AlMgB_{14}$ additive – a positive effect (a decrease in $d_{32}$ compared to the conditional "average" level) in the case of line 1 propellants, a negative effect in the case of line 2 propellants, and no effect for line 3 propellants.

Table 5 presents the main parameters – dimensionless mass of agglomerates $m_{80}$, burning rate $r$, mean size of agglomerates $D_{43}$, incompleteness of agglomerate combustion $\eta$, mean size of fine oxide particles $d_{32}$, as well as the "relative effect" showing the influence of the additive on each of the listed parameters under consideration. Definition of the relative effect for the abstract parameter $p$:

**Table 5.** The main parameters of the studied propellants and the influence of various additives on them

| Propellant | $m_{80}$ | $Z_{m80}$ | $r$, mm/s | $Z_r$ | $D_{43}$, μm | $Z_{D_{43}}$ | $\eta$ | $Z\eta$ | $d_{32}$, μm | $Z_{d_{32}}$ |
|---|---|---|---|---|---|---|---|---|---|---|
| P1 | 0.088 | 0 | 1.4 | 0 | 431 | 0 | 0.13 | 0 | 7.8 | 0 |
| P11 | 0.106 | 0.20 | 1.5 | 0.07 | 303 | –0.30 | 0.19 | 0.46 | 2.2 | –0.72 |
| P12 | 0.122 | 0.38 | 1.5 | 0.07 | 325 | –0.25 | 0.17 | 0.31 | 3 | –0.62 |
| P13 | 0.17 | 0.93 | 1 | –0.29 | 374 | –0.13 | 0.33 | 1.54 | 3 | –0.62 |
| P14 | 0.16 | 0.81 | 1 | –0.29 | 522 | 0.21 | 0.24 | 0.85 | 6.8 | –0.13 |
| P15 | 0.103 | 0.16 | 1.1 | –0.21 | 399 | –0.07 | 0.10 | –0.23 | 2.1 | –0.73 |
| P2 | 0.042 | 0 | 1.8 | 0 | 254 | 0 | 0.13 | 0 | 2.4 | 0 |
| P21 | 0.173 | 3.08 | 2.6 | 0.44 | 326 | 0.28 | 0.44 | 2.38 | 3.3 | 0.38 |
| P22 | 0.193 | 3.55 | 2.4 | 0.33 | 396 | 0.56 | 0.37 | 1.85 | 2 | –0.17 |
| P23 | 0.054 | 0.27 | 1.5 | –0.17 | 258 | 0.02 | 0.15 | 0.15 | 2.1 | –0.12 |
| P24 | 0.041 | –0.04 | 1.8 | 0 | 278 | 0.09 | 0.07 | –0.46 | 2.1 | –0.12 |
| P25 | 0.07 | 0.66 | 1.6 | –0.11 | 274 | 0.08 | 0.05 | –0.62 | 2.1 | –0.12 |
| P3 | 0.039 | 0 | 1.6 | 0 | 262 | 0 | 0.10 | 0 | 2.1 | 0 |
| P31 | 0.053 | 0.36 | 2 | 0.25 | 217 | –0.17 | 0.14 | 0.40 | 2.2 | 0.05 |
| P32 | 0.083 | 1.14 | 2.2 | 0.38 | 200 | –0.24 | 0.19 | 0.90 | 2 | –0.05 |
| P33 | 0.069 | 0.78 | 1.7 | 0.06 | 257 | –0.02 | 0.18 | 0.80 | 2.1 | 0 |
| P34 | 0.063 | 0.62 | 1.8 | 0.12 | 232 | –0.11 | 0.06 | –0.40 | 2.1 | 0 |
| P35 | 0.043 | 0.11 | 1.7 | 0.06 | 258 | –0.02 | 0.2 | 1 | 2.1 | 0 |

*Note*. Errors of values: $m_{80}$ – 0.02 (abs.), $r$ – 0.1 mm/s (abs.), $D_{43}$ – 22 μm (abs.), $\eta$ – 7% (rel.), $d_{32}$ – 10% (rel.).

$$Z_p = \frac{\left(p_{\text{for propellant with additive}} - p_{\text{for base propellant}}\right)}{p_{\text{for base propellant}}},$$

where $p$ is $m_{80}$, $r$, $D_{43}$, $\eta$, or $d_{32}$.

The presented results show that:

1. For propellants of lines 1 and 3, the studied additives lead to a decrease in the mean size of $D_{43}$ agglomerates, with the exception of propellant P14 with the additive $(NH_4)_2TiF_6$. The greatest effect of reducing the mean $D_{43}$ is observed for the $AlMgB_{14}$ additive and is $Z_{D_{43}} = -0.30$ (propellant P11). A good result is also given by the $TiB_2$ additive (the effect is $Z_{D_{43}} = -0.25$ and $Z_{D_{43}} = -0.24$ for propellants P12 and P32, respectively). For propellants of line 2, no additive leads to a decrease in the mean size of agglomerates.

2. The studied additives lead to an increase in the mass of agglomerates in most cases, with the exception of the additive $(NH_4)_2TiF_6$ when introducing it into the base propellant P2. However, even in this case the effect is insignificant, $Z_{m_{80}} = -0.04$ For propellant P24.

3. Additives $AlMgB_{14}$ and $TiB_2$ increase the burning rate of all propellants. Additives $Ca_3(PO_4)_2$, $(NH_4)_2TiF_6$, $NH_4BF_4$ increase the burning rate only in propellants of line 3. The maximum effect of increasing the rate is observed in propellant P21 with the additive $AlMgB_{14}$ and is $Z_r = 0.44$.

4. For propellants of lines 1 and 2 additive $Ca_3(PO_4)_2$ reduces the incompleteness of combustion $\eta$. The effects are $Z_\eta = -0.23$ (propellant P15) and $Z_\eta = -0.62$ (propellant P25, and this is maximum effect). For propellants of lines 2 and 3 the value $\eta$ reduces additive $(NH_4)_2TiF_6$, effects $Z_\eta = -0.46$ (P24) and $Z_\eta = -0.40$ (P34).

5. The effect of additives on the $d_{32}$ size of fine particles could not be studied. As a trend, it can be said that propellants of line 1 with large AP generate larger oxide particles compared to propellants of lines 2 and 3 with medium AP. The characteristic particle sizes $d_{32}$ are approximately 3 μm and 2 μm, respectively.

Table 6 formally summarizes the results obtained. The (+) sign in a cell denotes a positive effect, the (–) sign denotes a negative effect, and (0) denotes no effect. The (0) sign also stands in cases of a weak effect, when its value is less than the error of the parameter under

**Table 6.** Qualitative influence of additives on the parameters under consideration

| Additive | Propellant | $m_{80}$ | $r$ | $D_{43}$ | $\eta$ | $d_{32}$ | Propellant | $m_{80}$ | $r$ | $D_{43}$ | $\eta$ | $d_{32}$ | Propellant | $m_{80}$ | $r$ | $D_{43}$ | $\eta$ | $d_{32}$ | ***S*** |
|---|---|---|---|---|---|---|---|---|---|---|---|---|---|---|---|---|---|---|---|
| $AlMgB_{14}$ | P11 | – | 0 | + | – | + | P21 | – | + | – | – | – | P31 | – | + | + | – | 0 | **5** |
| $TiB_2$ | P12 | – | 0 | + | – | + | P22 | – | + | – | – | + | P32 | – | + | + | – | 0 | **6** |
| $(NH_4)_2TiF_6$ | P13 | – | – | + | – | + | P23 | – | – | 0 | – | + | P33 | – | 0 | 0 | – | 0 | **3** |
| $NH_4BF_4$ | P14 | – | – | – | – | + | P24 | 0 | 0 | 0 | + | + | P34 | – | + | + | + | 0 | **6** |
| $Ca_3(PO_4)_2$ | P15 | – | – | + | + | + | P25 | – | – | 0 | + | + | P35 | – | 0 | 0 | – | 0 | **5** |

*Note.* Positive effects (marked+): reduction of agglomerate mass, increase of burning rate, reduction of agglomerate sizes, reduction of combustion incompleteness, reduction of oxide particle size

consideration. The cells of the table with a positive effect are shaded. The last column of the table is the S (scores) parameter, the total number of "points" scored by a particular additive. The parameter is numerically equal to the sum of the "+" signs in the row of Table 6. As can be seen, the most effective in terms of the totality of the parameters studied turned out to be $NH_4BF_4$ additives, $TiB_2$ and $AlMgB_{14}$. Features of the substance $NH_4BF_4$ – high fluorine content. The $NH_4BF_4$ molecule contains about 72% fluorine, and in the molecule $(NH_4)_2TiF_6$ approximately 58% fluorine. This suggests the influence of the element F on the processes occurring during combustion. A feature of $TiB_2$ and $AlMgB_{14}$ powders is their high dispersion. Both powders were obtained by plasma recondensation [49], so their particles are mainly submicron in size.

## 6. CONCLUSION

The effect of the modifying additives titanium diboride $TiB_2$, aluminum and magnesium boride $AlMgB_{14}$, ammonium titanium (IV) fluoride $(NH_4)_2TiF_6$, ammonium tetrafluoroborate $NH_4BF_4$, calcium phosphate 3-substituted $Ca_3(PO_4)_2$ on the combustion parameters at a pressure of 0.35 MPa was investigated for the composite propellant consisting of aluminum ASD-4 as a fuel (≈20%), ammonium perchlorate as an oxidizing agent (≈60%) and an active binder based on MPVT (≈20%). The mass fraction of additives in the propellant is about 2% over 100%. In the experiments, the burning rate of propellant samples was measured using video recording and characteristics of condensed combustion products, by the quenching and sampling particles in a liquid. By analyzing the sampled particles, the mass, size and incompleteness of combustion of aluminum agglomerates larger than 80 μm, as well as the sizes of small (2–80 μm) oxide particles were determined. As a result, it was revealed how exactly each of the listed additives affects the determined parameters. The effect was assessed from the standpoint of increasing the burning rate, reducing the mass, size and incompleteness of combustion of agglomerates, as well as reducing the size of small particles. It was noted that the additives have a stronger effect on propellant with coarse AP (500–630 μm) than on propellants with medium AP (180–250 μm). The studied additives can be arranged in the following row in descending order of the totality of registered positive effects:

$$NH_4BF_4 = TiB_2 > AlMgB_{14} = Ca_3(PO_4)_2 > (NH_4)_2TiF_6.$$

Despite some positive effects, none of the five additives provides a simultaneous significant reduction in both the size and mass of agglomerates. At the same time, the analysis, although based on a limited set of experimental data (one pressure level of 0.35 MPa, one type of binder), demonstrated the fundamental possibility of additives influencing the selected combustion parameters. Therefore, work on finding new additives capable of reducing the intensity of agglomeration should be continued. Highly dispersed powders of substances with a high fluorine content seem promising.

## FUNDING

This work was financed by the Ministry of Science and Higher Education of the Russian Federation within the framework of the state task (FWGF-2021–0001). No additional grants to carry out or direct this particular research were obtained.

## CONFLICT OF INTEREST

The authors of this work declare that they have no conflicts of interest.

## REFERENCES


1. B. P. Zhukov, editor. *Energetic condensed systems. Brief Encyclopedic Dictionary*. (Yanus-K, Moscow, 2000). [In Russian]
2. S. F. Sarner *Propellant Chemistry*. (New York, 1966).
3. V. I. Tsutsuran, N. V. Petrukhin, Gusev S. A. *Military-technical analysis of the state and prospects for the development of rocket propellants*. (MO RF, Moscow, 1999). [In Russian]
4. E. M. Nurullayev *Main characteristics of composite solid propellants and areas of their application. 2nd ed*. (Infra-Inzheneriya, Moscow, Vologda, 2021). [In Russian]
5. Yu. V. Frolov, P. F. Pokhil, V. S. Logachev, Combust Explos Shock Waves. **8**, 2, 168. (1972).
6. A. G. Korotkikh, I. V. Sorokin, E. A. Selikhova, V. A. Arkhipov, Russ. J. Phys. Chem. B. **14**, 4, 600. (2020). https: // doi.org/ 10.1134/S1990793120040089
7. A. G. Korotkikh, I. V. Sorokin, V. A. Arkhipov, Russ. J. Phys. Chem. B. **16**, 2, 259. (2022). https: // doi.org/ 10.1134/S1990793122020075
8. V. D. Gladun, Yu.V Frolov et al., *Agglomeration of a part of powdered metal during combustion of mixed condensed systems* [preprint]. (Institut khimicheskoy fiziki AN SSSR, Chernogolovka, 1977). [In Russian]
9. P. F. Pokhil, V. M. Maltsev, V. S. Logachev et al., Combust Explos Shock Waves. **7**, 1, 43 (1971).
10. Yu. V. Frolov, B. E. Nikolsky, Combust Explos Shock Waves. **19**, 5, 625 (1983).
11. V. A. Babuk, V. P. Belov, V. V. Khodosov et al., Combust Explos Shock Waves. **21**, 3, 287 (1985).
12. K. Jaraman, S. R. Chakravarthy, R. Sarathi, Combust Explos Shock Waves. **46**, 1, 21 (2010).
13. O. G. Glotov, V. E. Zarko V. V. Karasev et al., *Comb. and detonation. 28th International Annual Conference of ICT*. (Karlsruhe, Germany, 1997), Report **75**.
14. V. E. Zarko, O. G. Glotov, Science and Tech. of Ener. Materials. **74**, 6, 139 (2013).
15. Y. G. Liu, X. Tian, L. Yin et al., Combust Explos Shock Waves. **58**, 2, 190 (2022).
16. V. A. Babuk, D. I. Kuklin, S. Yu. Naryzhny et al., Combust Explos Shock Waves. 59, 2, 236 (2023).
17. O. G. Glotov, Combust Explos Shock Waves. 42, 4, 436 (2006).
18. I. Yu. Gudkova, I. N. Zyuzin, D. B. Lempert, Russ. J. Phys. Chem. B. **14**, 2, 302. (2020). https: // doi.org/ 10.1134/S1990793122010067
19. I. Yu. Gudkova, I. N. Zyuzin, D. B. Lempert, Russ. J. Phys. Chem. B. **16**, 1, 58. (2022). https: // doi.org/ 10.1134/S1990793120020062
20. T. I. Gorbenko, Vestnik SibSAU im. M. F. Reshetneva. **23**, 2, 173 (2009). [In Russian]
21. V. N. Popok, V. N. Khmelev *Composite condensed chemical propellants based on ammonium nitrate. Principles of layout and properties*. (Izd-vo Altayskogo gos. tekhnicheskogo un-ta im. I. I. Polzunova, Biysk, 2014). [In Russian]
22. G. V. Sakovich, V. A. Arkhipov, A. B. Vorozhtsov et al., Izvestiya TGU. **314**, 3, 18 (2009). [In Russian]
23. G. Ya. Pavlovets, V. Yu. Meleshko, B. I. Larionov et al., Khim. fizika i mezoskopiya. **8**, 1, 53 (2006). [In Russian]
24. V. D. Gladun, Yu. V. Frolov, L. Ya. Kashporov, Combust Explos Shock Waves. **13**, 5, 596 (1977).
25. V. N. Popok, A. P. Vandel, A. Yu. Kolesnikov, Butlerovskiye soobshcheniya. **36**, 11, 58 (2013). [In Russian]
26. V. N. Popok, N. I. Popok, Yu. A. Pivovarov, Butlerovskiye soobshcheniya. **49**, 15 (2017). [In Russian]
27. X. Liu, W. Ao, H. Liu et al., Propellants, Explos., Pyrotech. **42**, 3, 260 (2017).
28. U. R. Nair, R. Sivabalan, Gore G. M. et al., Combust Explos Shock Waves. **41**, 2, 121 (2005).
29. S. Lal, R. J. Staples, J. M. Shreeve, Chem. Eng. J. **468**, 143737, (2023).
30. V. A. Babuk, V. P. Belov, G. G. Shelukhin, Combust Explos Shock Waves. **17**, 3, 264 (1981).
31. E. W. Price, R. K. Sigman, J. R. Sambamurthi et al. *Behavior of aluminum in solid propellant combustion*. (AFOSR-TR-82–0964, Georgia Institute of Technology, 1982).
32. L. L. Breiter, L. Ya. Kashporov, V. M. Maltsev et al., Combust Explos Shock Waves. **7**, 2, 186 (1971).
33. Y. Aly, M. Schoenitz, E. L. Dreizin, Comb. Flame. **160**, 835 (2013). http://dx.doi.org/10.1016/j.combust-flame.2012.12.011.
34. W. Ao, Z. Fan, L. Lu et al., Comb. Flame. **220**, 288 (2020). https://doi.org/10.1016/j.combust-flame.2020.07.004.

35. W. He, J. Y. Lyu, D. Y. Tang et al., Comb. Flame. **221**, 441 (2020).
36. A. Yu. Dolgoborodov, Combust Explos Shock Waves. **51**, 1, 86 (2015).
37. D. A. Yagodnikov *Ignition and combustion of powdered metals in gas-dispersed media*. (MGTU im. N. E. Baumana, Moscow, 2018). [In Russian]
38. O. G. Glotov, D. A. Yagodnikov, V. S. Vorob'ev et al., Combust Explos Shock Waves. **43**, 3, 320 (2007).
39. V. G. Shevchenko, D. A. Eselevich, N. A. Popov et al., Combust Explos Shock Waves. **54**, 1, 58 (2018).
40. V. Rosenband, A. Gany Intern. J. Energetic Mater. Chem. Propuls. **6**, 2, 143 (2007).
41. E. Shafirovich, P. E. Bocanegra, C. Chanveau et al. Proc Combust Inst. **30**, 2, 2055 (2005).
42. T. A. Andrzejak, E. Shafirovich, A. Varma Combust. Flame. **150**, 60 (2007).
43. E. A. Lebedeva, I. L. Tutubalina, A. Valtsifer et al. Combust Explos Shock Waves. **48**, 6, 694 (2012).
44. J. Y. Lyu, G. Xu, H. Zhang et al. Fuel. 356, 129587 (2024).
45. A. G. Korotkikh, O. G. Glotov, V.A Arkhipov. et al. Combust. Flame. **178**, 195 (2017). https: //doi.org/10.1016/j.combust-flame.2017.01.004
46. W. Q. Pang, L. T. DeLuca, X. Z. Fan, et al. Combust. Flame. **220**, 157 (2020).
47. K. Tejasvi, V. V. Rao, Y. PydiSetty et al. Combust Explos Shock Waves. **57**, 2, 203 (2021).
48. L. T. DeLuca, L. Galfetti, F. Severini et al. Combust Explos Shock Waves. **41**, 6, 680 (2005).
49. Sh. L. Guseynov, S. G. Fedorov *Nanopowders of aluminum, boron, aluminum and silicon borides in high-energy materials*. (Torus Press, Moscow, 2015). [In Russian]
50. F. K. Bulanin, A. E. Sidorov, N. I. Poletaev et al. Combust Explos Shock Waves. **57**, 2, 190 (2021).
51. L. D. Romodanova, P. F. Pokhil Combust Explos Shock Waves. **9**, 2, 195 (1973).
52. Aerosol Calculator Program // http: // www. cheresources.com/che-links/content/particle-technology/aerosol-calculator-program. 2012. URL: http: // cires.colorado.edu/jimenez-group/Reference/aerocalc.zip (accessed on: 22.03.2024).
53. O. G. Glotov, V. E. Zarko, V. V. Karasev, Combust Explos Shock Waves. **36**, 146 (2000).
54. V. A. Babuk, V. A. Vasilyev, M. S. Malachov J. Propul. Power. **15**, 6, 783 (1999).
55. V. A. Babuk, V. A. Vassilyev, V. V. Sviridov Combust Sci Technol. **163**, 261 (2001).
56. J. K. Sambamurthi, E. W. Price, R. K. Sigman AIAA Journal, **22**, 8, 1132 (1984)
57. K. P. Kutsenogii *Candidate of dissertation tech. Sci.* (Institute of Chemical Kinetics and Combustion Siberian Branch of the Russian Academy of Sciences, Novosibirsk, 1970). [In Russian]
58. L. Ya. Gradus *A Guide to Dispersion Analysis Microscopy.* (Khimiya, Moscow, 1979). [In Russian]
59. T. D. Fedotova, O. G. Glotov, V. E. Zarko Propellants, Explos. Pyrotech. **32**, 2, 160 (2007).
60. W. Pang, L. T. De Luca, X. Fan et al. *Boron-Based Fuel-Rich Propellant: Properties, Combustion, and Technology Aspects.* (CRC Press, 2019).
61. O. G. Glotov, I. V. Sorokin, A. A. Cheremisin Combust Explos Shock Waves. **59**, 6, 752 (2023).